Water Research 217 (2022) 118420

Contents lists available at ScienceDirect

Water Research

journal homepage: www.elsevier.com/locate/watres

Exploring the use of flow cytometry for understanding the efficacy of disinfection in chlorine contact tanks

Ryan Cheswick [a,b], Andreas Nocker [c], Graeme Moore [b], Bruce Jefferson [a], Peter Jarvis [a,*]

[a] Cranfield University, Bedford, MK43 0AL, UK
[b] Scottish Water, Castle House, Dunfermline, KY11 8GG, UK
[c] IWW Water Centre, Mlheim an der Ruhr, Germany

ARTICLE INFO

Keywords:
Disinfection
Microorganisms
Chlorine
Drinking water
Flow cytometry

ABSTRACT

A pilot scale chlorine contact tank (CCT) with flexible baffling was installed at an operational water treatment plant (WTP), taking a direct feed from the outlet of the rapid gravity filters (RGF). For the first time, disinfection efficacy was established by direct microbial monitoring in a continuous reactor using flow cytometry (FCM). Disinfection variables of dose, time, and hydraulic efficiency (short circuiting and dispersion) were explored following characterisation of the reactor's residence time distributions (RTD) by tracer testing. FCM enabled distinction to be made between changes in disinfection reactor design where standard culture-based methods could not. The product of chlorine concentration (C) and residence time (t) correlated well with inactivation of microbes, organisms, with the highest cell reductions (N/N_0) reaching <0.025 at $Ct_{\bar{x}}$ of 20 mg.min/L and above. The influence of reactor geometry on disinfection was best shown from the Ct_{10}. This identified that the initial level of microbial inactivation was higher in unbaffled reactors for low Ct_{10} values, although the highest levels of inactivation of 0.015 could only be achieved in the baffled reactors, because these conditions enabled the highest Ct_{10} values to be achieved. Increased levels of disinfection were closely associated with increased formation of the trihalomethane disinfection by-products. The results highlight the importance of well-designed and operated CCT. The improved resolution afforded by FCM provides a tool that can dynamically quantify disinfection processes, enabling options for much better process control.

1. Introduction

Disinfection by chlorine remains the final barrier in most drinking water treatment systems before water enters distribution. The efficacy of disinfection is typically designed using the product of the chlorine concentration (C) and the disinfection contact time (t), known as the Ct. The desired flow conditions in chlorine contact tanks (CCT) used for disinfection should be as close to plug flow as possible to ensure the full contact time is experienced by all portions of the water being treated. True plug flow is seldom achieved due to incompatible geometries (the ideal is a narrow channel with a length to width (L/W) ratio greater than 40) or increased dispersion due to turbulence caused by friction effects with the walls and baffles (Rauen et al., 2012). Non-ideal flow conditions are detrimental to the performance of CCTs, leading to short-circuiting and unwanted recirculation within the reactor. Short circuiting occurs when a proportion of the fluid by-passes much of the available reactor volume and exits the reactor sooner than the theoretical hydraulic retention time (HRT). In turn this can lead to insufficient inactivation of microorganisms, as that portion of the flow would not receive the desired Ct. Recirculation leads to excessive contact time in 'dead zones' and promotes short circuiting due the reduction in the effective operating proportion of the tank. The importance of having as close to ideal flow conditions in CCTs has been demonstrated previously using both empirical and theoretical testing (Angeloudis et al., 2014a; Teixeira et al., 2008; Rauen et al., 2008). The effectiveness of a CCT can be described with hydraulic efficiency indicators (HEIs) that are derived from residence time distributions (Teixeira et al., 2008).

HEIs can also be derived via computational fluid dynamics (CFD), a simulation approach that does not require physical experimental testing and avoids potential scaling issues (Rauen et al., 2012; Angeloudis et al., 2014a, b, 2016; Goodarzi et al., 2020). However, calibration of CFD models is required and it is preferential to carry out physical testing to best calibrate the simulations (Falconer, 1986). Estimates of disinfection efficacy in CCTs have been made using established disinfection

* Corresponding author.
E-mail address: p.jarvis@cranfield.ac.uk (P. Jarvis).

https://doi.org/10.1016/j.watres.2022.118420
Received 8 October 2021; Received in revised form 29 March 2022; Accepted 30 March 2022
Available online 6 April 2022

inactivation kinetic calculations (Chick-Watson law) and disinfection by-product (DBP) formation kinetics (Brown et al., 2011; Angeloudis et al., 2014a). However, these experiments did not record real microbial inactivation rates. This is an important consideration given that organisms of different characteristics have a unique residence time distribution in tanks, in addition to having different inactivation kinetics (Asraf-Snir and Gitis, 2011). As a result, research is ongoing as to which model best describes the transport of particles (in this case bacteria) through the reactor and the most appropriate disinfection kinetic model that should be used in CFD approaches (Angeloudis, 2014). To date, no papers have reported the use of direct microbial monitoring of environmental microbes to assess disinfection variables in CCTs.

The traditional approach of monitoring microbial inactivation during disinfection is by using indicator organisms. This becomes challenging at the low bacterial concentrations presented at disinfection stages, resulting in limited detection and a high error on measurements (Cheswick et al., 2019). In addition, pathogen surrogates (coliforms, *Escherichia coli* or *Enterococci*) are not suitable performance indicators due to the rare occurrence of these organisms before and after disinfection as well as their high sensitivity to chlorine. An alternative is to monitor heterotrophic bacteria using heterotrophic plate counting (HPC). These bacteria are typically abundant in drinking water and may have higher recovery rates following disinfection, making them a more suitable process indicator (Hijnen, 2008). However, chlorination can lead to the loss of bacterial culturability without destroying the cell, which can lead to skewed representations of inactivation (Berney et al., 2006). In addition, it has been concluded that HPC measurements do not provide any information on the hygienic quality of the water (Van Nevel et al., 2017).

An alternative approach is the use of flow cytometry (FCM) for quantifying the autochthonous bacterial population in drinking water. There have been many demonstrations of the benefits of this technique over traditional culture based methods (Hoefel et al., 2005; Berney et al., 2007; Ho et al., 2012; Van Nevel et al., 2017; Cheswick et al., 2019). Successful application has been shown in laboratory studies investigating various oxidant kinetics (Ramseier et al., 2010; Ding et al., 2019; Cheswick et al., 2020) and real-time monitoring of biocide kinetics (heat and ciprofloxacin exposure) (Arnoldini et al., 2013). This methodology has also gained significant attention as a tool for assessing operational water treatment plants (WTPs) (Helmi et al., 2014; Cheswick et al., 2019), distribution systems (Gillespie et al., 2014; Nescerecka et al., 2018) and in water reuse (Safford and Bischel, 2018; Whitton et al., 2018). However, there is a knowledge gap in the ability of FCM to be used for optimisation and design of disinfection processes.

The aim of this work was to determine the role that FCM can play in developing our understanding of disinfection in continuous flow chlorine contact tanks and establish relationships between hydraulic efficiency indicators and inactivation. This was achieved by comparing traditional microbial monitoring parameters (HPC and indicator organisms) with that of total and intact cells measured by FCM in a pilot scale CCT reactor with various baffling arrangements and flow rates treating real water. The inactivation achieved was compared to other disinfection parameters, including formation of disinfection by-products (DBPs) in chlorinated water. The novelty of the present work was to therefore use FCM to directly determine disinfection efficacy, establishing the role that advanced microbial monitoring can play in future development and monitoring of chlorine disinfection.

2. Materials and methods

2.1. Experimental conditions

A pilot scale CCT was located at an operational WTP in Scotland, UK. The WTP was a conventional surface water treatment plant (Fig. 1a). The pilot plant was supplied with water from the WTP following filtration and was representative of real water presented to disinfection. The reactor mimicked a typical longitudinal serpentine baffled CCT with the option of removing baffles to change the hydraulic conditions (Fig. 1b). The CCT was 1.8 m long, 1.2 m wide with a water of depth 0.42 m. The minimal channel width was 0.23 m when fully baffled and

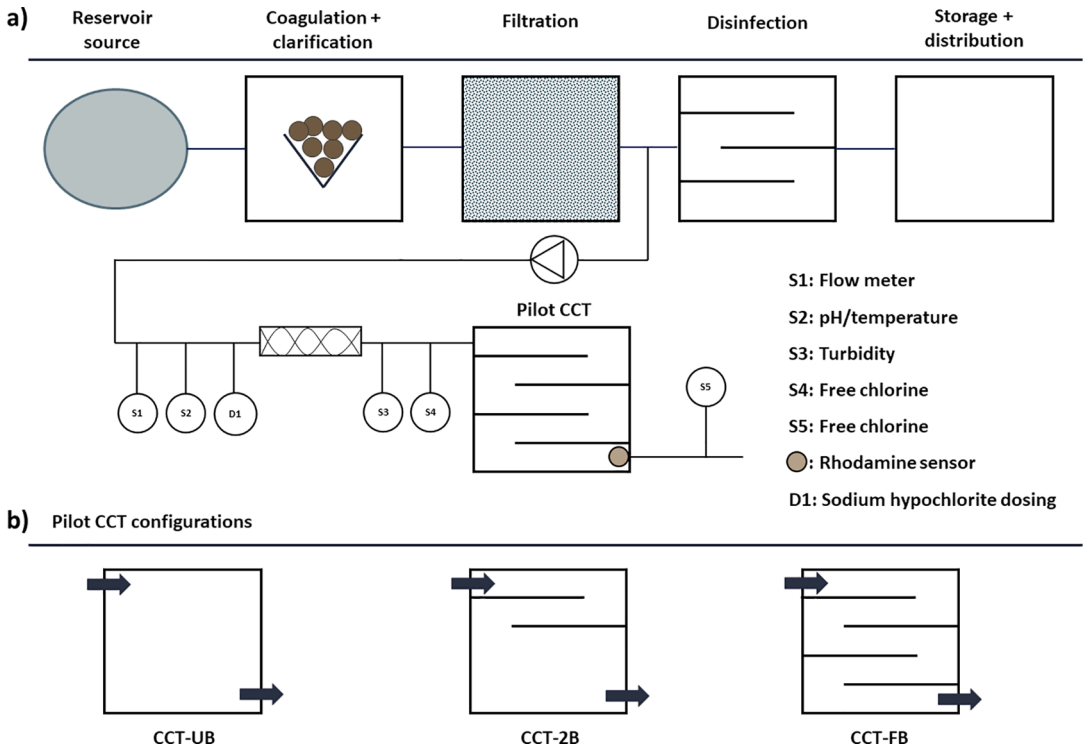

Fig. 1. Schematic drawing of the water treatment plant used to supply the filtered water for this study and arrangement of sensor and dosing points (a), and pilot CCT baffle configurations (b).

1.3 m when unbaffled. Flow rates were varied using a pump supply from the filtered water channel and monitored using a flowmeter (Siemens SITRANS F M MAG, Nordborg, Denmark). Sodium hypochlorite was dosed via a dosing pump (Grundfus Digital Dosing Control (DDC), Grundfos Pumps Ltd, Bedfordshire, UK) prior to an inline static mixer. Downstream of this mixer was a turbidity metre (AMI Turbiwell, Swan Analytical USA Inc, Illinois, USA) and a free chlorine monitor (Hach Cl17, Manchester, UK). At the outlet of the tank was a rhodamine sensor with internal data logger (CYCLOPS-7, Turner Designs, California, USA) for tracer testing and a second free chlorine monitor. A programmable logic controller (PLC) allowed for outlet chlorine concentrations to be controlled.

Tests were carried out over a range of flow rates to provide theoretical HRT (T) of between 10 and 40 min. Two chlorine doses were applied (0.5 and 1 mg/L Cl_2) and three baffling conditions, incorporating an un- (UB), partially (2B) and fully baffled (FB) reactor geometry, with 0, 2 and 4 baffles, respectively. Conditions were selected to cover a range of operational chlorine concentrations and residence times as well as considering best to worst baffling arrangements (Table 1). Sampling took place once a period of three theoretical HRT had expired and the outlet chlorine concentration was stabilised to allow complete turnover of the water and an equilibrium to be reached for each condition tested. 500 mL samples were taken from a sample tap in the outlet pipework, immediately at the exit of the tank. The diameter of this outlet pipe was 10 cm and hence the sample taken was assumed to be representative of the bulk flow. Chlorine was quenched from the sample using sodium thiosulphate, with a subsample taken for analysis on the day of collection. For each condition, three replicate samples were taken, with data reported as the arithmetic mean of the samples.

2.2. Tracer experiments

Tracer experiments were carried out using the pulse trace methodology with Rhodamine WT (Acros Organics, Geel, Belgium). A submersible fluorometer at a maximum resolution of $\Delta t = 3$ s was used for the detection of the rhodamine trace. Each tracer experiment lasted for a minimum of three theoretical retention times and subsequent tests were only carried out after a fourth retention time had passed to allow complete turnover of the water within the reactor. The tracer was added to the inlet of the reactor via a manual syringe injection of rhodamine WT solution (20 mL at 35 mg/L, mass of rhodamine added = 7000 μg). This injection time was within that recommended by Marske and Boyle (1973) and was no more than 1/50th of the reactor retention time. To effectively describe the residence time distribution (RTD) the results were normalised using the E-curve method (Levenspeil, 2012). The mean residence time ($\overline{tx}$) was calculated from the area under the Concentration (C)/ time (t) curve, Equation 1:

$$\overline{tx} = \frac{\sum_0^\infty (t \cdot C \cdot \Delta t)}{\sum_0^\infty (C \cdot \Delta t)}$$

This curve was transformed into the E curve, such that the area under the curve was unity. Using the tracer mass (M) and reactor flow rate (Q), Equation 2:

$$E = C \cdot \frac{Q}{M}$$

The E curve was then translated into an $E(\theta)$ curve from Equation 3:

$$E(\theta) = \bar{x} \cdot E$$

Finally, the normalised time (θ) was calculated from the measured time (t) and the theoretical retention time (T), Equation 4:

$$\theta = \frac{t}{T}$$

The RTD variance (σ^2) was calculated from Equation 5:

$$\sigma^2 = \frac{\sum t^2 \cdot C \cdot \Delta t}{\sum C \cdot \Delta t} - \theta^2$$

The variance and the mean residence time was then used to calculate the dispersion index of the RTD curve (σ_t^2), Equation 6:

$$\sigma_t^2 = \frac{\sigma^2}{\bar{x}^2}$$

This normalisation allows for interpretation of the hydraulic performance across variable flow rates. Time specific tracer parameters were recorded and HEIs (Table 2) were calculated using the RTD results and were classified from poor to excellent based on criteria from AWWA (2006) and Angeloudis et al., 2014a (SI Table S1).

2.3. Water quality measurements

HPCs were determined by mixing 1 mL of sample into 18 mL of molten Yeast Extract Agar (YEA) (Oxoid, ThermoFisher Scientific, UK). These plates were duplicated with one incubated at 37 °C for 48 h (HPC 37 °C) and the second at 22 °C for 72 h (HPC 22 °C), in accordance with standard methods. The determination of coliforms and *E. coli* was carried out by membrane filtration. 100 mL of sample was passed through a 0.45 μm membrane filter. Plates were incubated at 30 °C for 4 h and then 37 °C for 14 h.

FCM analysis for determination of intact (ICC) and total cell counts (TCC) was carried out using an adapted method as described previously (Gillespie et al., 2014) with the amendment of a 25 μL undiluted sample volume in accordance with the rapid method described by Van Nevel et al., 2013. For measurement of TCC, SYBR Green I (10, 000 X stock, cat. no. S-7567; Life Technologies Ltd, Paisley, UK) was diluted with

Table 1
Experimental conditions and reactor parameters.

CCT configuration	No. of baffles (n)	Length to width (L:W) ratio	Reactor volume (m^3)	Flow rates tested (L/min)/HRT (mins)	Chlorine doses (mg/L)	Reynolds number (Re)*
UB	0	1.5	0.924	92.4 (10)	0.5 1.0	3020
				46.2 (20)		1510
				23.1 (40)		755
2B	2	23.4	0.924	92.4 (10)	0.5 1.0	5000
				46.2 (20)		2500
				23.1 (40)		1250
FB	4	39.1	0.924	92.4 (10)	0.5 1.0	5757
				46.2 (20)		2879
				23.1 (40)		1439

UB – unbaffled; 2B – 2 baffles; FB – fully baffled.
*Reynolds number >2000 for open channel flow is considered turbulent.
Reynolds number calculated from $Re = 4*V*Hr/\upsilon$, where V = flow velocity (m/s), Hr = Hydraulic radius (m), υ = kinematic viscosity (m^2/s). Hr was calculated from A/P_w, where A = flow cross sectional area (m^2) and P_w = wetted perimeter (m).

Table 2
Commonly used time specific and hydraulic efficiency indicators (HEIs) for describing residence time distributions (RTDs) of tracer tests (adapted from (Wang and Falconer, 1998; Teixeira et al., 2008).

Class	Name	Description
Time specific parameters	T	Theoretical hydraulic retention time
	t_i	Time for initial tracer front to pass the outlet
	t_{10}	Time taken for 10% mass of tracer to pass the outlet
	t_{50}	Time taken for 50% of the tracer mass to pass the outlet
	t_P	The maximum tracer concentration arrival time
	$t_{\bar{x}}$	Tracer mean.
Short circuiting indices	t_{10}/T	Relative time taken for 10% of the tracer to pass. Standard value for assessing short circuiting within reactors.
	t_{90}/T	Relative time taken for 90% of the tracer to pass. A measure of the recirculation within the tank
	$t_{\bar{x}}/T$ V%	Relative tracer mean. Used to identify if there are dead spaces/stagnation within the reactor in conjunction with T. If $t_{\bar{x}} = T$ then all of the tank volume is in use by the fluid. If $t_{\bar{x}} < T$ then some of the vessel is not being used (indicating dead regions) and finally if $t_{\bar{x}} > T$ this indicates there is recirculation within the reactor holding the tracer back. The dead volume in the reactor: $(1- t_{\bar{x}}/T)*100$
Mixing indexes	Morril index, Mo	The Morril index is the ratio between the time taken for 90 and 10% of the tracer to pass the outlet (t_{90}/t_{10})
	Dispersion index, σ_t^2	The dispersion index is a measure of the variance of the RTD function (σ^2/T)
	t_{90}-t_{10}	The time elapsed between 10 and 90% of the tracer leaving the vessel.

dimethyl sulphoxide (DMSO; Fisher Scientific, Fair Lawn, NJ) to a working stock concentration of 100x, of which 2 μL were added to sample volumes of 200 μL (final SYBR Green I concentration: 1x). For measurement of ICC, dye mixtures were made containing five-parts of 100 X SYBR Green I and one-part propidium iodide (PI) (1 mg/mL, corresponding to 1.5 mM; cat. nr. P3566; Life Technologies Ltd., Paisley, UK). 2.4 μL of this dye mixture was added to 200 μL water samples in 96 well plates (final concentrations of SYBR Green I: 1 X, final concentration of PI: 3 μM). Following the addition of the dyes the samples were incubated in a plate incubator for 30 min at 30 °C in the dark. Following incubation, 25 μL samples were analysed using a BD Accuri C6 flow cytometer equipped with a 488 nm solid state laser (Becton Dickinson UK Ltd, Oxford, UK) in accordance with the rapid method described by Van Nevel et al., 2013. The FCM was calibrated with Spherotech validation beads (Becton Dickinson UK Ltd, Oxford, UK) to ensure that the instrument was operating within acceptable limits as stated by the manufacturer. Green fluorescence was collected in the FL1 channel at 533 nm (FL1) and red fluorescence in the FL3 channel at 670 nm (FL3) with the trigger set on the green fluorescence. No compensation was used. TCC and ICC were quantified using a fixed gate as used previously for detection of bacteria present in natural water sources (Gatza et al., 2013; Cheswick et al., 2020). All data were reported back above the reported limit of quantification of $<1 \times 10^2$ cells and well below the upper limit of quantification (1×10^7 cells). The frequency of microorganisms contained in this gate after staining with SYBR Green I or SYBR Green I/PI formed the basis for calculations of TCC or ICC (per mL). Data was processed using the Accuri C6 software.

Trihalomethane (THM) concentrations were measured in samples exiting the CCT following chlorination following methods reported elsewhere (Golea et al., 2019). Chlorine was quenched with excess sodium thiosulphate following sampling. The total THM concentration (tTHM) was measured using gas chromatography spectrometry with headspace injection using the standard USEPA 551 method (USEPA, 1998). A minimum of 7 injections were undertaken for each measurement.

3. Results and discussion

3.1. General water quality

The water quality entering the pilot remained stable throughout the trial with respect to pH (pH = 6.4 ± 0.1), temperature (12.7 ± 0.5 °C) and DOC (2.7 ± 0.3 mg/L) such that a consistent chlorine demand of 0.18 ± 0.05 mg/L was presented (SI Table S2). The consistency of the water quality enabled the inactivation data to be directly related to the two components of chlorine dose and hydraulic conditions (White, 2010; Haas and Engelbrecht, 1980). The culture based bacterial counts in the inlet had significant variation. For example, the HPC 22 °C had an average of 40 CFU/mL with a minimum of non-detectable and a maximum of >300 CFU/mL. The HPC 37 °C had even lower counts with most samples returning non-detect samples and a maximum of 4 CFU/mL. In contrast, the FCM ICC remained relatively consistent throughout the trial ($5.20 \times 10^5 \pm 3.36 \times 10^4$ cells/mL), with cell concentration values that were between 3 and 4 orders of magnitude higher than seen for the culture-based method. Only three HPC positive detections were observed after chlorine addition from the samples taken at the reactor outlet (maximum CFU/mL = 3). All other samples ($n = 53$) were reported as non-detectable. These results highlight the poor resolution afforded by traditional culture based methods for assessment of log reductions across water treatment processes. This impact is particularly seen for disinfection due to the low number of cells going into and out of the process. FCM, on the other hand, was able to detect significant cell concentrations in both the inlet and outlet (see inactivation section), allowing much better assessment of the true efficacy of disinfection.

3.2. Hydraulic performance

The hydraulic performance of the pilot CCT was improved as baffling increased, approaching idealised plug flow (PF) conditions. This highlights the importance of considering the hydraulic efficiency in Ct calculations. The unbaffled condition (UB) showed a large spike of tracer leaving the reactor shortly after injection due to streaming across the tank. This was followed by a long tail of the trace caused by the large recirculation zone in the centre of the tank (example for HRT of 20 min shown in Fig. 2). This profile was typical of an unbaffled reactor and similar to that of a continuously stirred reactor (CSTR) rather than the desired PF conditions (Levenspiel, 2012).

Summary RTD values show how the baffles improve hydraulic efficiency for each of the flow rates (SI Figure S1 and Table S3). To demonstrate, analysis of the RTD for the UB reactor at a theoretical HRT=20 mins gave a t_{10}/T of 0.09 showing in this case that 10% of the tracer had exited the reactor within 1.8 min of the injection. Approaches to quantify mixing in the tank using the dispersion index ($\sigma_t^2 = 0.735$) and the Morril index (Mo = 15.45) resulted in values classified as *poor* by the HEI descriptors. With the introduction of two baffles in the tank the RTD profile improved. The tracer front was held back from short circuiting the reactor rapidly, and the tail of the RTD was shortened. The introduction of these channels reduced the dispersion and improved the value of the dispersion index to a level associated with an HEI descriptor of *acceptable* ($\sigma_t^2 = 0.188$). Similarly, the Morril Index improved from an HEI descriptor of *compromising* to one classified as *acceptable* (Mo = 2.15) (Table S3). Short circuiting was reduced ($t_{10}/T = 0.47$) but was still evident as a result of 50% of the tank volume remaining un-baffled, which allowed for streaming in the final compartment. It was evident from visual observation of the tracer that recirculation was occurring in this final section of the tank (Fig. 3). When fully baffled, the RTD resembled a normally distributed curve, centred around the theoretical residence time ($\theta = 1$). Short circuiting was significantly reduced to a value associated with an HEI descriptor of *excellent* for serpentine CCT

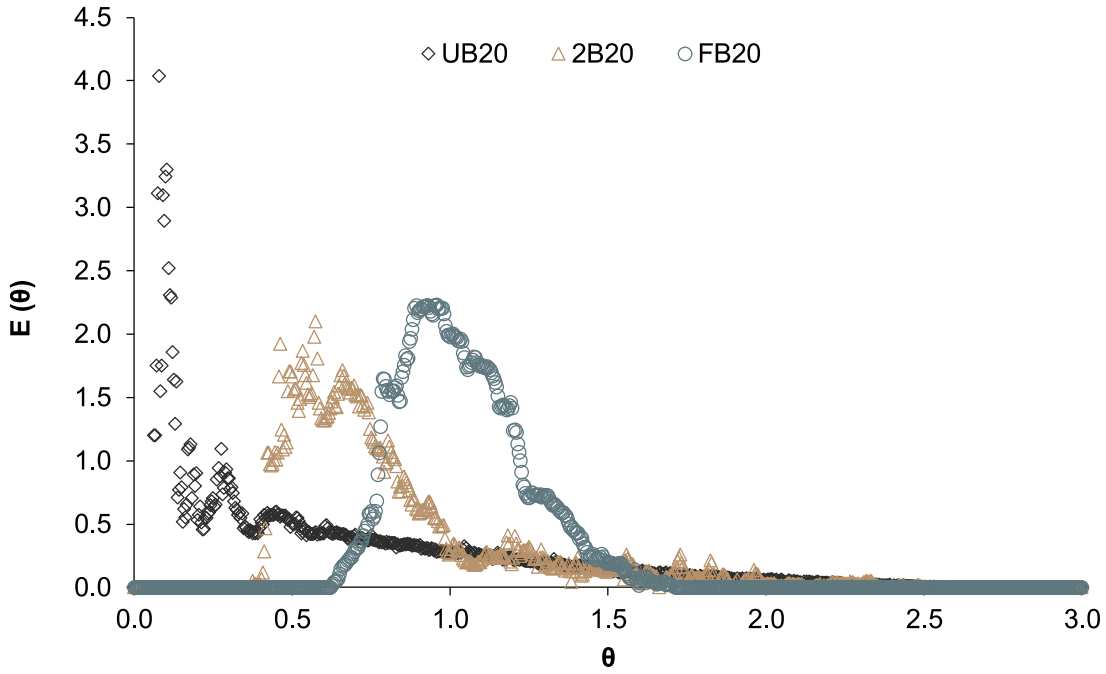

Fig. 2. Normalised residence time distributions (RTDs) for each of the baffling conditions at a theoretical retention time of 20 min. UB20 = unbaffled at a theoretical HRT of 20 mins; 2B20 = 2 baffles at HRT of 20 mins; FB20 = fully baffled at 20 mins HRT.

Fig. 3. Images of the rhodamine tracer in the pilot CCT captured over the theoretical residence time. Inlet and outlet locations are indicated by arrows and are in the same location for each test.

reactors (t_{10}/T = 0.79), and dispersion was brought down to a level commensurate with the descriptor *excellent* (σ_t^2 = 0.034). This was visually confirmed by a compact tracer block moving through the tank (Fig. 3 and video files available here: doi.org/10.17862/cranfield.rd.16773220).

Comparison of the hydraulic efficiency of the different baffle arrangements was assessed at three HRTs and compared in relation to t_{10}/T, σ_t^2 and Mo (SI Figure S1 and Table S3). The normalised HEIs indicated only small variation as a function of HRT as illustrated through the t_{10}/T ranges which were 0.09–0.13, 0.46–0.49 and 0.79–0.89 for the unbaffled, two baffles and fully baffled tanks, respectively. Importantly, only the fully baffled arrangement delivered acceptable hydraulic conditions for all flow rates investigated. Whilst partial baffling improved the hydraulic performance relative to the unbaffled reactor, appropriate conditions were only seen for specific flow rates, revealing a loss of resilience in the system. This distinction between baffling arrangements was also seen for the two mixing indices (σ_t^2 and Mo), although the separation was less clearly defined between the two-baffle reactor and

the fully-baffled system for the Mo. The t_{90}/T increased substantially from 1.1 to 1.7 for the unbaffled reactor as the residence time decreased, evidence of the long tail of tracer as the flow rate through the reactor reduced (SI Figure S2). Less distinction was seen for t_{90}/T in the baffled systems. Overall, baffling had a larger impact on HEI's than the flow rate, a finding supported by Zhang et al. (2014) who also saw that the t_{10}/T and Morril index were unaffected by changing flow rates. For the fully baffled contactor, no dead zones were evident (although $t_{\bar{x}}$ was $>T$, indicating that there was some recirculation of the tracer at the outlet of the tank, an effect that was exaggerated at the longer HRT of 40 mins). For the two-baffle contact tank, the dead volume remained similar at the different HRT, between 19.2 and 24.2%. For unbaffled reactors, the volume of the dead zone in the reactor increased from 32.0, 38.3 and 71.3% with theoretical HRT of 10, 20 and 40, respectively.

The comparison of the HEIs indicate that the different tank arrangements were best distinguished by the t_{10}/T. The two mixing HEIs should not be considered in isolation, as an *acceptable* σ_t^2 and *excellent* Mo could be classified as *compromising* with regards to the short-circuiting index (t_{10}/T), a situation seen for the two-baffle chlorination reactor. When considering mixing, the σ_t^2 has been reported to be the most suitable mixing index for assessment of CCTs as it considers the whole RTD function (Teixeira et al., 2008). This was consistent with the observations seen here, where better distinction was seen between the mixing in the two-baffled system compared to the fully baffled reactor.

3.3. Inactivation efficiency

In order to assess the efficacy of disinfection, samples were taken from the inlet and outlet of the CCT for each experimental assessment of baffling and HRT condition (Fig. 4a). At the inlet to the CCT there was a median HPC count of 26CFU/mL, with the minimum reported value as 'non-detectable' and a maximum reported as >300 CFU/mL. As noted, nearly all samples from the outlet were reported as non-detectable, thus preventing assessment of removal efficacy across the CCT using culture-based methods. This variation is typical of that seen when using total viable count methods and is routinely seen in operational practice, where more than 92% of samples in chlorinated water are typically returned as non-detects (Cheswick et al., 2019). Irrespective of the disinfection conditions, only a single coliform colony was detected by standard microbiological analysis (Table S2). No *E. coli* were detected throughout the entirety of the study. These findings reinforce the challenge of microbial monitoring of disinfection processes when using traditional methods.

In contrast, the results from FCM analysis carried out on the same sample offered more insights into process performance, providing data that has not been previously available. At the inlet to the CCT there was a median TCC observed of 613,440 cells/mL, reaching a maximum of 867,200 cells/mL and a minimum of 510,160 cells/mL. The median ICC at the inlet was 86% of the TCC median at 527,960 cells/mL showing that a proportion of cells had compromised membrane integrity prior to disinfection. At the outlet of the reactor there was a much wider variation in the TCC than those observed at the inlet. The median TCC was 5% lower in the outlet than the TCC at the inlet (579,600 cells/mL) whilst the range of TCC went from 23,600 to 835,200 cells/mL. As cells were oxidised by chlorine in the CCT, many cellular structures will be sufficiently damaged such that they will no longer interact with the fluorescing dyes. As a result, this will reduce the total number of cells counted, particularly in systems where microbes had been exposed to longer Cts (represented by the long bottom whisker in Fig. 4b). The median ICC was much lower than for the inlet at 25,280 cells/mL (range 7080 to 39,920 cells/mL). Importantly, this enabled the importance of baffling and the connection between inactivation and hydraulic indicators to be re-examined through a more detailed lens. The results also show the suitability of using ICC to determine the efficacy of chlorine-based disinfection. Chlorine is a non-selective oxidant that damages cellular components, notably the cell membrane. Damage to cell membranes is strongly associated with reduced viability of both pure cultured and environmental bacteria (Nocker et al., 2017). No relationships were found between the concentrations of HPC and FCM cell counts for either ICC or TCC. This is a result consistent with previous studies, highlighting the differences in microbial populations that are quantified by these different methods (Van Nevel et al., 2017; Cheswick et al., 2019).

To elucidate the impacts of flow on the efficacy of disinfection, the

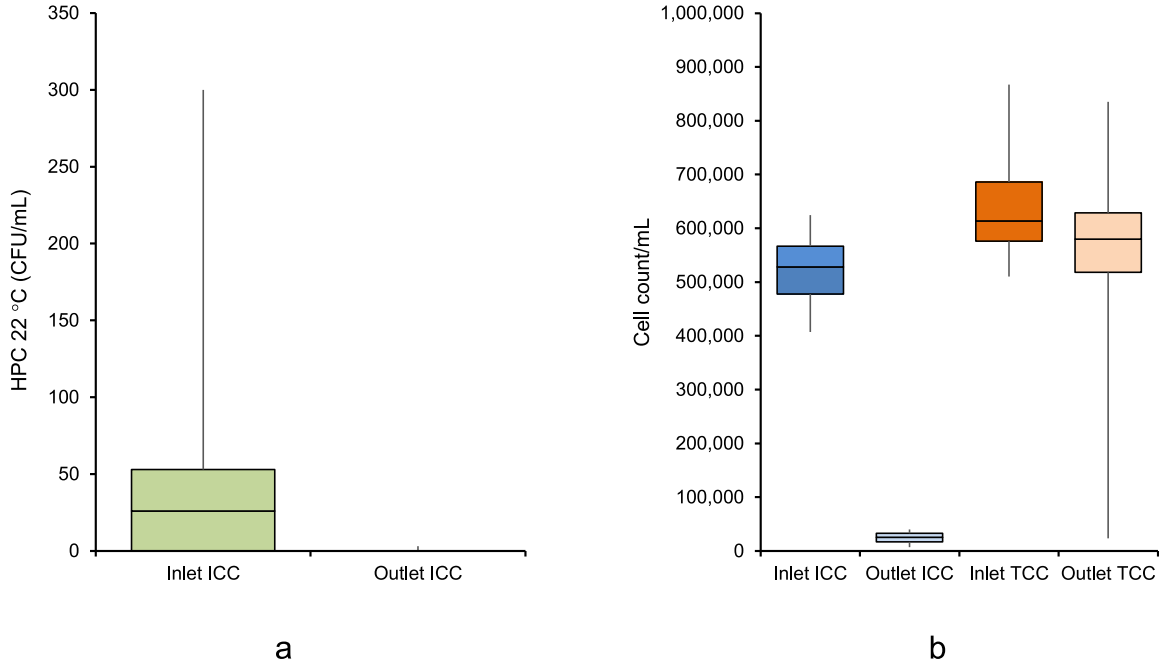

Fig. 4. Box whisker plots for inlet ($n = 53$) and outlet ($n = 53$) microbiological monitoring throughout the trial period. This data has been pooled into one sample set irrespective of the disinfection conditions for comparison of methods. Heterotrophic plate counts (HPC) are shown (a) and flow cytometric data for intact and total cells are included (b).

cell inactivation was correlated to the various HEI adjusted Ct values using the mean residence time ($t_{\bar{x}}$), the 10th (t_{10}) and 90th (t_{90}) percentile residence time (Fig. 5). Cell inactivation was considered by determining the cell survival ratio, defined as the proportion of ICC in samples taken from the outlet of the contact tank relative to those seen in the inlet. The survival ratio was therefore the inverse of cell inactivation. During these tests, the range of survival ratios were between 0.08 and 0.015. For the highest survival ratio of 0.08, this represented cell inactivation of 92%, while the lowest survival ratio of 0.015 was equivalent to inactivation of 98.5%. Higher levels of cell inactivation was seen with increasing Ct_x (Fig. 5a). The steepest drop in cell survival was seen at low Ct_x values up until 10 mg.min/L, with around 4% of the cells measured as intact. At higher Ct the increase in cell inactivation slowed, reaching between 1.5 and 2% cell survival at Ct >20 mg.min/L. The surviving cells represent the bacteria that were more resistant to chlorine disinfection, attributable to heterogenous bacterial populations present in any system which have varying tolerance to oxidation (Cerf, 1977). Those bacteria surviving chlorine disinfection have been identified previously as spore forming species, acid-fast, partially acid-fast and Gram-positive bacteria, linked to their thicker cell walls (Norton and LeChavallier, 2000; WHO, 2022).

While the baffling arrangements clearly led to differences in the HEIs, there was little to distinguish between the cell survival ratios for the different baffling arrangements when the $Ct_{\bar{x}}$ was considered (Fig. 5a). Instead, the inactivation was more linked to the ability of the reactor to be able to deliver longer residence times. These conditions were predominately observed when the highest degree of baffling was applied and dead zones in the reactor were minimised. However, best practice for disinfection considers the more conservative Ct_{10} which considers the first 10% of the residence time distribution leaving the CCT (Angeloudis et al., 2014a). The highest bacterial inactivation could only be achieved for the highest Ct_{10} values, and these could only be achieved when baffling was in place (summarised for Ct_{10} in Table 3). The maximum Ct_{10} achievable for the different baffling arrangements was 3.3 mg.min/L for the UB reactor and 31.9 mg.min/L for the FB reactor (Fig. 6b). The lowest cell survival ratios of 0.015 were only seen when the Ct_{10} was >15 mg.min/L, conditions that could only be achieved with baffling.

For the UB conditions, there was an initially steep drop in the survival ratio from 0.075 to 0.035 as the Ct_{10} increased from 0.3 to 3.6 mg.min/L (the maximum value achievable). In comparison, the 2B and FB reactors followed a more shallow inactivation profile. To illustrate, inactivation only declined from 0.075 to 0.060 as the Ct_{10} increased from 0.3 to 3.6 mg.min/L. As noted, however, these baffled reactors were able to achieve the highest residence times which was when the highest inactivation was seen.

When the Ct_{90} was considered, there was a bigger difference in the inactivation between reactor geometries as the Ct_{90} went beyond 20 mg.min/L (Fig. 5c). For example, at a Ct_{90} of 42.7 mg.min/L for the UB reactor, the inactivation was 0.041 while at a similar Ct_{90} of 46 mg.min/L for the FB reactor, the inactivation was only 0.018.

As similar picture was observed when THM formation in the reactors were considered, with values ranging from 6 to 16 μg/L. While the DBP concentrations were low relative to the drinking water quality standards of Europe and North America (Evlampidou et al., 2020; Chen et al., 2019), the highest THM concentrations were associated with the longest residence times (Fig. 6a-c). As seen for microbial inactivation, most discrimination between reactor layout was seen when the Ct_{10} was considered, showing a more rapid increase in formation with residence time for the UB reactor (Fig. 6b). Slower rates of increase were seen for the FB followed by the 2B reactors, although the highest THM concentration values were seen for these systems, due to their ability to be able to deliver longer contact times. The $Ct_{\bar{x}}$ and Ct_{90} did not provide a clear distinction between baffling arrangements with respect to DBP formation (Figs. 6a and c).

These results support the use of the Ct_{10} as an HEI that can provide the most appropriate discrimination between reactor types, providing insight into how short-circuiting impacts on disinfection efficacy and disinfection by-product formation. The results presented here are interesting because they demonstrate a higher initial level of

Table 3
Summary of the cell inactivation as determined by flow cytometry for disinfection in chlorine contact tanks with different baffling arrangements, chlorine concentrations and residence time at t_{10}.

Baffling	T (min)	t_{10} (min)	C (mg/L)	Ct_{10} (min)	Survival ratio N/N_0	Log inactivation -log (N/N_0)
FB	10	8.0	0.50	4.00	0.057	1.246
			0.93	7.44	0.040	1.396
	20	15.8	0.46	7.27	0.054	1.270
			0.97	15.33	0.022	1.648
	40	35.7	0.52	18.56	0.029	1.533
			0.89	31.77	0.018	1.746
2B	10	4.6	0.45	2.07	0.080	1.095
			1.00	4.60	0.063	1.202
	20	9.4	0.47	4.42	0.060	1.224
			0.93	8.74	0.035	1.453
	40	19.6	0.50	9.80	0.031	1.507
			0.97	19.01	0.016	1.792
UB	10	1.3	0.47	0.61	0.077	1.112
			0.93	1.21	0.063	1.199
	20	1.8	0.47	0.85	0.058	1.237
			0.97	1.75	0.048	1.321
	40	3.4	0.57	1.94	0.034	1.462
			0.96	3.26	0.041	1.387

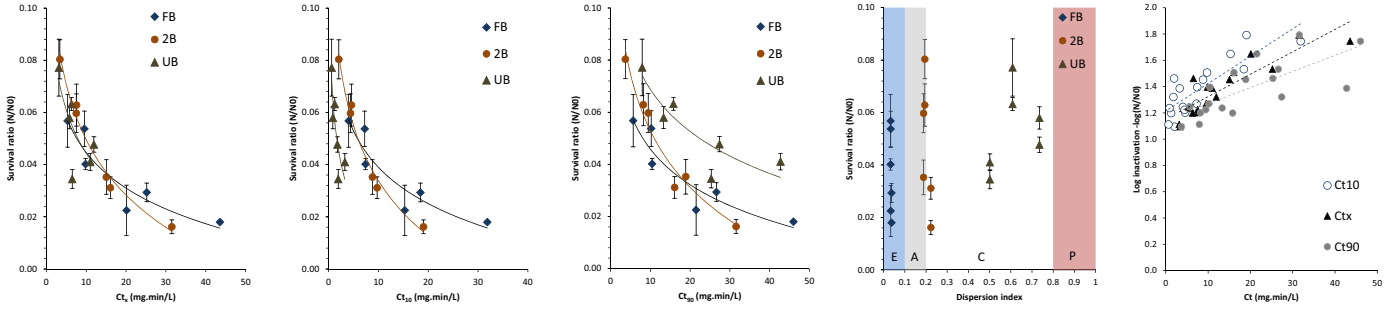

Fig. 5. Survival ratios for intact cell counts calculated from the inlet and outlet of the CCT against three HEI converted Ct values, the $Ct_{\bar{x}}$ (a), Ct_{10} (b), Ct_{90} (c) and the Dispersion Index (σ^2), where shaded regions represent areas of Excellent (E), Acceptable (A), Compromised (C) and Poor (P) hydraulic performance (d); log inactivation (-Log(N/N_0) plot for all experimental conditions for the Ct_{10} and $Ct_{\bar{x}}$ (e).

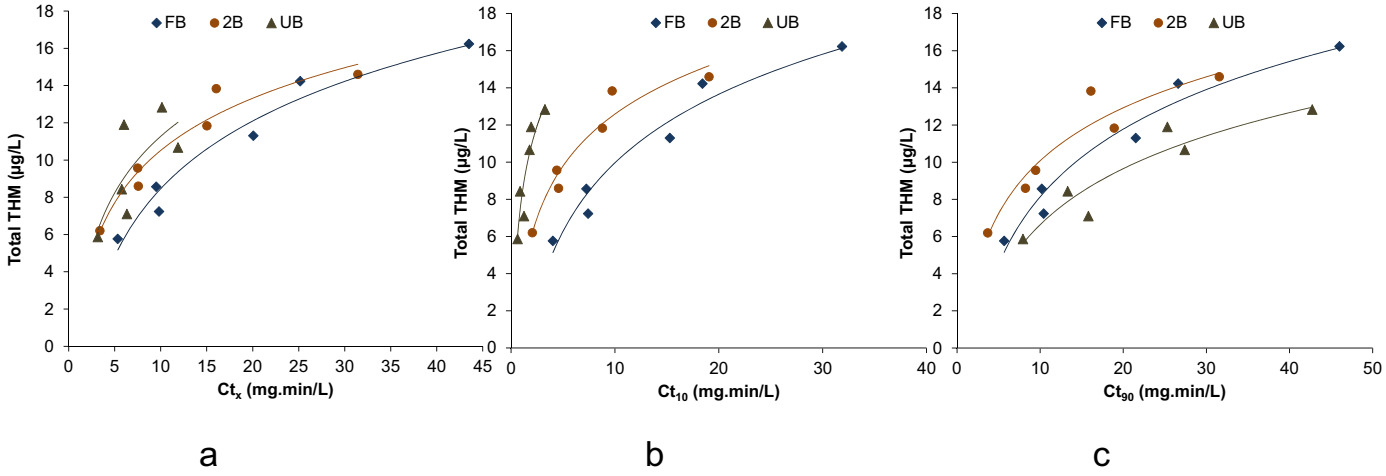

Fig. 6. Total THM concentration at the outlet of the CCT with increasing Ct, for the $Ct_{\bar{x}}$ (a), Ct_{10} (b) and Ct_{90} (c).

inactivation and DBP formation for unbaffled reactors in comparison to fully and partially baffled systems at low Ct_{10} values (<5 mg.min/L). It is posited that this reflects the change in the flow pattern when operating the CCT without baffles, where the RTD profile deviates significantly away from plug flow. As a result, a significant proportion of the water exiting the tank has had an extended period of contact time in the reactor for both inactivation and chemical reactions to take place. This was a view supported by the significantly higher dead volumes and recirculation zones present in UB reactors. These dead zones have previously been modelled to be hotspots for increased DBP formation (Angeloudis et al., 2014a; Angeloudis et al., 2016) and presumably this would also be the case for high levels of disinfection, assuming that residual chlorine is still present. However, the fact that a larger proportion of the flow has had a relatively short contact time as a result of short-circuiting when compared to the baffled reactors means that the highest inactivation values could not be achieved. This is particularly relevant when considering the range of microbes present in environmental systems that will have different tolerances to chlorine and hence will require longer contact for inactivation (Ridgway and Olson, 1982). Similarly, under conditions of significant short circuiting, there will be large volume of water in the CCT with an extended residence time, providing opportunities for increased formation of disinfection by-products

With regards to the dispersion index, an *excellent* HEI value ($\sigma_t^2 = 0.1$) did not guarantee consistently similar levels of disinfection, with survival ratios between 0.018–0.057, showing the dominance of the Ct on microbial inactivation. In the present case, the partially baffled reactor produced a similar level of performance to that seen for the FB. This was posited to be due to the high susceptibility to chlorine of the organisms present. It would be expected that the FB reactor with the best hydraulic indicators would handle microbes with increased chlorine tolerance much better.

The log inactivation rates observed here did not achieve the 2-log (99%) reduction (Fig. 6e) that is typically considered for effective disinfection (WHO, 2017). In the present study, a maximum log reduction of 1.79 was observed for Ct >19 mg.min/L from an initial cell concentration of 6.38×10^5 TCC/mL. In comparison, laboratory assessment of chlorine disinfection using FCM to assess bacterial inactivation saw up to 1-log inactivation at a Ct of 20 mg.min/L at an initial bacterial concentration of 14×10^7 TCC/mL (Ramseier et al., 2010). In this case the authors showed that FCM, which measures membrane integrity, had lower inactivation than culture-based methods that have been used to traditionally define inactivation rates, regardless of the oxidant used, and were not able to achieve 2-log reduction. The present results extend this understanding further, confirming similar observations for continuous systems, more akin to real disinfection practice. The implication of these results being that FCM provides a more conservative measure of disinfection efficacy such that adjustment of target log reductions may be required if it is to be used as a validation indicator. The difference relates to the fact that FCM measures membrane integrity, whereas traditional methods reflect culturability. For example, *E. coli* cells have been reported to lose culturability well before the loss of membrane integrity (Lisle et al., 1999; Ramseier et al., 2010; Nocker et al., 2017). This observed loss of culturability supports the concept of chlorination inducing a viable but not culturable (VBNC) state for the bacterial cells (Wang et al., 2010) and explains why all but three HPC samples returned a 'non-detectable' results in the current study, while significant numbers of intact cells were still measured by FCM.

4. Future perspectives of FCM as monitoring technique for disinfection efficacy

Methods such as FCM for total bacterial counts should not be considered an alternative for measurement of indicator organisms as part of compliance monitoring as no clear correlation exists between the two (Cheswick et al., 2020). FCM should be viewed as a complimentary tool, enabling the efficacy of CCT to be viewed through a different, more sensitive lens that enables closer to real time measurement and avoids the more limited insights that results from the predominately non-detectable results obtained from culture-based approaches. It should also be acknowledged that, while used for regulatory monitoring, the bacteria that are cultured during HPC tests are largely non-pathogenic and hence there is no clear-cut public health risk, particularly for healthy individuals (WHO, 2003). Indicator organisms that are indicative of faecal contamination of drinking water have a strong rationale for inclusion but are fortunately rarely found in properly treated water.

The application of FCM provided new insights in relation to differences in inactivation rates for increasing contact time that were dependent on reactor configuration, with more rapid initial reduction in cell survival seen in unbaffled reactors for equivalent low values of Ct_{10}. To the authors' knowledge, this is an observation that has not been previously reported. The practical consequence of this is not to advocate the use of unbaffled reactors because the highest inactivation could only be observed at the longer Cts when baffling was added. Instead, it shows the importance of considering the whole bacterial population when considering disinfection. In reactors with significant short-circuiting, bacteria which have low chlorine tolerance can still be easily killed, but those which have a higher tolerance may pass straight through the

reactor. This became clearer when equivalent Ct_{90} values were considered, where the highest inactivation was only seen in baffled systems. Further, the results showed the merits of even partial baffling where significant inactivation was still possible. The implication of this relates to existing CCT, where a significant number in operation around the world have little to no baffling. Adaptation of these existing tanks to incorporate some degree of baffling will have a significant impact on inactivation and offer the possibility of low cost upgrading of existing CCTs. This can be achieved relatively simply and effectively using retrofitted baffle plates and curtains (Nasyrlayev et al., 2020).

The FCM approach quantifies a fuller representation of the native microbial community, importantly including the non-culturable organisms. This provides measurable numbers with sufficient resolution to enable effective exploration of design and operating impacts. In addition, the method was able to reveal hitherto unexplored impacts related to the breadth of chlorine tolerances within environmental populations, allowing for greater understanding of variation both within the same water supply and between different water sources. Importantly, it enables us to move beyond the use of surrogate organisms (such as *E. coli*, total coliforms and *Enterococci*) which are known to exhibit a particularly high susceptibility to chlorine at Ct levels of between 0.01–1 mg. min/L (Stanfield, 2005). Moreover, FCM is a fast, practical technique that can be used as a routine measurement in practice (Cheswick et al., 2020) to compliment more advanced techniques around species and strain identification. Direct microbial monitoring could be used more effectively alongside modelling approaches to demonstrate the efficacy of new innovations to CCT design and operation that have been developed by CFD (Angeloudis et al., 2016; Bruno et al., 2021). Numerical modelling of disinfection and by-product formation remains a challenge due to the dependency on kinetic models that are not equipped to deal with the complexities of real systems. Hence the methods described in this work have the potential to significantly help in the development of more accurate and functional numerical based modelling of disinfection processes.

FCM has the potential to offer significant value with regards to optimisation, process investigations and route cause analysis. With the development of online FCM and the increasing uptake in the application of this approach for monitoring treatment process dynamics (Besmer et al., 2016; Favere et al., 2020) it is likely that FCM could be applied in near real time for active disinfection monitoring.

5. Conclusions

The work aimed to explore the use of flow cytometry to understand if it could provide fresh insights into the design or operation of chlorine contact tanks. The results provided novelty in presenting the first set of experimental data to explore the use of FCM for CCT, alongside comparative data based on traditional microbial monitoring and hydraulic efficiency parameters. Importantly, FCM provides positive data throughout, negating the problems associated with large datasets of non-detectable results that occur when using culture-based approaches. This empowers fresh consideration into the performance of CCT both in terms of design and performance monitoring. This is most apparent in the comparison between the impact of baffling on hydraulic efficiency indicators and inactivation. Clear distinction was observed with the former but was not always seen in the case of the latter and thus suggests the need to re-evaluate the role of baffling on organism inactivation. Interestingly, the unbaffled systems initially provided more rapid decrease in cells at low Ct values compared to the baffled system. This was attributed to the higher proportion of dead zones and recirculation that prevailed in the unbaffled system. Ultimately, however, the highest inactivation rates were connected with the ability of the reactor to be able to deliver the longest Ct_{10}. This was delivered most consistently with the fully baffled system. However, partial baffling also had the ability to deliver similar inactivation levels. The importance of this relates to the potential for enhancement of existing systems with achievable modifications, such as insertion of curtains to provide some degree of baffling.

These new insights offered here show the importance of monitoring the whole native population. In practice, regular monitoring of inactivation is required to ensure that the diversity of organisms present is captured and to ensure that the Ct can be tailored to the specific requirements. The measurement of the survival of intact cells enabled accurate derivation of inactivation from a real water source containing only environmentally relevant bacteria.

Declaration of Competing Interest

None.

Acknowledgements

The authors gratefully thank Scottish Water for part-funding this research and allowing access to their water treatment works sites for sample collection and analysis. The financial and practical support of EPSRC (under the STREAM programme EP/G037094/1) is also appreciatively acknowledged.

Data underlying this paper can be accessed at: https://doi.org/10.17862/cranfield.rd.16773220.

Supplementary materials

Supplementary material associated with this article can be found, in the online version, at doi:10.1016/j.watres.2022.118420.

References

Angeloudis, A., 2014. Numerical and Experimental Modelling of Flow and Kinetic Processes in Serpentine Disinfection Tanks. Cardiff University.
Angeloudis, A., Stoesser, T., Falconer, R.A., 2014b. Predicting the disinfection efficiency range in chlorine contact tanks through a CFD-based approach. Water Res. 60, 118–129.
Angeloudis, A., Stoesser, T., Falconer, R.A., Kim, D, 2014a. Flow, transport and disinfection performance in small- and full-scale contact tanks. J. Hydroenviron. Res. (July), 1–14.
Angeloudis, A., Stoesser, T., Gualtieri, C., Falconer, R., 2016. Contact tank design impact on process performance. Environ. Model Assess. 21, 563–576.
Arnoldini, M., Heck, T., Blanco-Fernández, A., Hammes, F., 2013. Monitoring of dynamic microbiological processes using real-time flow cytometry. PLoS One 8 (11), e80117.
Asraf-Snir, M., Gitis, V., 2011. Tracer studies with fluorescent-dyed microorganisms—a new method for determination of residence time in chlorination reactors. Chem. Eng. J. 166 (2), 579–585.
AWWA, 2006. Water Chlorination /Chloramination Practices and Principles, Second. American Water Works Association.
Berney, M., Hammes, F., Bosshard, F., Weilenmann, H.-U., Egli, T., 2007. Assessment and interpretation of bacterial viability by using the LIVE/DEAD BacLight Kit in combination with flow cytometry. Appl. Environ. Microbiol. 73 (10), 3283–3290.
Berney, M., Weilenmann, H.U., Egli, T., 2006. Flow-cytometric study of vital cellular functions in Escherichia coli during solar disinfection (SODIS). Microbiology 152 (6), 1719–1729.
Besmer, M.D., Epting, J., Page, R.M., Sigrist, J.A., Huggenberger, P., Hammes, F., 2016. Online flow cytometry reveals microbial dynamics influenced by concurrent natural and operational events in groundwater used for drinking water treatment. Sci. Rep. 6, 38462.
Brown, D., Bridgeman, J., West, J.R., 2011. Understanding data requirements for trihalomethane formation modelling in water supply systems. Urban Water J. 8, 41–56.
Bruno, P., Di Bella, G., De Marchis, M., 2021. Effect of the contact tank geometry on disinfection efficiency. J. Water Process Eng. 41, 102035.
Cerf, O., 1977. Tailing of survival curves of bacterial spores. J. Appl. Bacteriol. 42, 1–19.
Chen, Y., Arnold, W.A., Griffin, C.G., Olmanson, L.G., Brezonik, P.L., Hozalski, R.M., 2019. Assessment of the chlorine demand and disinfection by-product formation potential of surface waters via satellite remote sensing. Water Res. 165, 115001.
Cheswick, R., Cartmell, E., Lee, S., Upton, A., Weir, P., Moore, G., Nocker, A., Jefferson, B., Jarvis, P., 2019. Comparing flow cytometry with culture-based methods for microbial monitoring and as a diagnostic tool for assessing drinking water treatment processes. Environ. Int. 130, 104893.
Cheswick, R., Moore, G., Nocker, A., Hassard, F., Jefferson, B., Jarvis, P., 2020. Chlorine disinfection of drinking water assessed by flow cytometry: new insights. Environ. Technol. Innov., 101032
Ding, W., Jin, W., Cao, S., Zhou, X., Wang, C., Jiang, Q., Huang, H., Tu, R., Han, S.-F., Wang, Q., 2019. Ozone disinfection of chlorine-resistant bacteria in drinking water. Water Res. 160, 339–349.

Evlampidou, I., Font-Ribera, L., Rojas-Rueda, D., Gracia-Lavedan, E., Costet, N., Pearce, N., Vineis, P., Jaakkola, J.J.K., Delloye, F., Makris, K.C., Stephanou, E.G., Kargaki, S., Kozisek, F., Sigsgaard, T., Hansen, B., Schullehner, J., Nahkur, R., Galey, C., Zwiener, C., Vargha, M., Righi, E., Aggazzotti, G., Kalnina, G., Grazuleviciene, R., Polanska, K., Gubkova, D., Bitenc, K., Goslan, E.H., Kogevinas, M., Kogevinas, M., Villanueva, C.M., 2020. Trihalomethanes in Drinking Water and Bladder Cancer Burden in the European Union, 128. Environmental Health Perspectives, 017001.

Falconer, R.A., 1986. A theoretical and hydraulic model study of a chlorine contact tank. Proc. Inst. Civil Eng. (81), 255–276.

Favere, J., Buysschaert, B., Boon, N., De Gusseme, B., 2020. Online mmicrobial fingerprinting for quality management of drinking water: full-scale event detection. Water Res. 170, 115353.

Gillespie, S., Lipphaus, P., Green, J., Parsons, S., Weir, P., Juskowiak, K., Jefferson, B., Jarvis, P., Nocker, A., 2014. Assessing microbiological water quality in drinking water distribution systems with disinfectant residual using flow cytometry. Water Res. 65, 224–234.

Goodarzi, D., Abolfathi, S., Borzooei, S., 2020. Modelling solute transport in water disinfection systems: effects of temperature gradient on the hydraulic and disinfection efficiency of serpentine chlorine contact tanks. J. Water Process Eng. 37, 101411.

Haas, C.N., Engelbrecht, R.S., 1980. Chlorine dynamics during inactivation of coliforms, acid-fast bacteria and yeasts. Water Res. 14 (12), 1749–1757.

Helmi, K., Watt, Jacob, P, Ben-Hadj-Salah, I, Henry, Méheut, G., Charni-Ben-Tabassi, N, 2014. Monitoring of three drinking water treatment plants using flow cytometry. Water Sci. Technol.: Water Supply 14 (5), 850.

Hijnen, W.A.M., 2008. Elimination of Micro-Organisms in Water Treatment. KWR Watercycle Research Institute.

Ho, L., Braun, K., Fabris, R., Hoefel, D., Morran, J., Monis, P., Drikas, M., 2012. Comparison of drinking water treatment process streams for optimal bacteriological water quality. Water Res. 46 (12), 3934–3942.

Hoefel, D., Monis, P.T., Grooby, W.L., Andrews, S., Saint, C.P., 2005. Culture-independent techniques for rapid detection of bacteria associated with loss of chloramine residual in a drinking water system. Appl. Environ. Microbiol. 71 (11), 6479–6488.

Levenspeil, O., 2012. Tracer Technology. Springer Science and Business media.

Lisle, J.T., Pyle, B.H., McFeters, G.A., 1999. The use of multiple indices of physiological activity to access viability in chlorine disinfected Escherichia coli O157:H7. Lett. Appl. Microbiol. 29 (1), 42–47.

Marske, D.M., Boyle, J.D., 1973. Chlorine contact tank chamber deisng - a field evaluation. Water Sewage Works 120 (1), 70–77.

Nasyrlayev, N., Kizilaslan, M.A., Kurumus, A.T., Demirel, E., Aral, M.M., 2020. A perforated baffle design to improve mixing in contact tanks. Water 12, 1022.

Nescerecka, A., Juhna, T., Hammes, F., 2018. Identifying the underlying causes of biological instability in a full-scale drinking water supply system. Water Res. 135, 11–21.

Nocker, A., Cheswick, R., Dutheil de la Rochere, P.-.M., Denis, M., Léziart, T., Jarvis, P., 2017. When are bacteria dead? A step towards interpreting flow cytometry profiles after chlorine disinfection and membrane integrity staining. Environ. Technol. 38 (7), 891–900.

Norton, C.D., LeChavellier, M.W., 2000. A pilot study of bacteriological population changes through potable water treatment and distribution. Appl. Environ. Microbiol. 66 (1), 268–276.

Ramseier, M.K., Gunten, U.Von, Freihofer, P., Hammes, F, 2010. Kinetics of membrane damage to high (HNA) and low (LNA) nucleic acid bacterial clusters in drinking water by ozone, chlorine, chlorine dioxide, monochloramine, ferrate (VI), and permanganate. Water Res. 45 (3), 1490–1500.

Rauen, W., Lin, B., Falconer, R., Teixeira, E., 2008. CFD and experimental model studies for water disinfection tanks with low Reynolds number flows. Chem. Eng. J. 137 (3), 550–560.

Rauen, W.B., Angeloudis, A., Falconer, R.A., 2012. Appraisal of chlorine contact tank modelling practices. Water Res. 46 (18), 5834–5847.

Ridgway, H.F., Olson, B.H., 1982. Chlorine resistance patterns of bacteria from two drinking water distribution systems. Appl. Environ. Microbiol. 44 (4), 972–987.

Safford, H.R., Bischel, H.N., 2018. Flow cytometry applications in water treatment, distribution, and reuse: a review. Water Res. 151, 110–133.

Stanfield, G., 2005. A Review of Ct in Water Disinfection. Report Ref. No. 05/DW/02/37. UK Water Industry Research Ltd.

Teixeira, E.C., Ph, D., Siqueira, N., 2008. Performance assessment of hydraulic efficiency indexes. J. Environ. Eng. 134 (October), 851–859.

USEPA, 1998. National primary drinking water regulations: disinfectants and disinfection byproducts. U.S. Environmental protection agency. Fed. Regist. 63 (241), 69390–69476.

Van Nevel, S., Koetzsch, S., Proctor, C.R., Besmer, M.D., Prest, E.I., Vrouwenvelder, J.S., Knezev, A., Boon, N., Hammes, F., 2017. Flow cytometric bacterial cell counts challenge conventional heterotrophic plate counts for routine microbiological drinking water monitoring. Water Res. 113, 191–206.

Van Nevel, S., Koetzsch, S., Weilenmann, H., Boon, N., Hammes, F, 2013. Routine bacterial analysis with automated flow cytometry. J. Microbiol. Methods 94 (2), 73–76.

Wang, H., A Falconer, R, 1998. Simulating disinfection processes in chlorine contact tanks using various turbulence models and high-order accurate difference schemes. Water Res. 32 (5), 1529–1543.

Wang, Y., Claeys, L., Van Der Ha, D., Verstraete, W., Boon, N., 2010. Effects of chemically and electrochemically dosed chlorine on Escherichia coli and Legionella beliardensis assessed by flow cytometry. Appl. Microbiol. Biotechnol. 87 (1), 331–341.

White, 2010. In: Desiderio, Dominic, Nibbering, Nico (Eds.), White's Handbook of Chlorination and Alternative Disinfectants, 5th Edition. John Wiley & Sons Inc, New Jersey.

Whitton, R., Fane, S., Jarvis, P., Tupper, M., Raffin, M., Coulon, F., Nocker, A., 2018. Flow cytometry-based evaluation of the bacterial removal efficiency of a blackwater reuse treatment plant and the microbiological changes in the associated non-potable distribution network. Sci. Total Environ. 645, 1620–1629.

WHO, 2003. In: Bartram, J., Cotruvo, J., Exner, M., Fricker, C., Glasmacher, A. (Eds.), Heterotrophic plate counts and drinking water safety. John WHO.

WHO, 2017. Drinking water parameter cooperation project. Support to the revision of Annex 1 Council Directive 98/83/EC on the Quality of Water Intended for Human Consumption (Drinking Water Directive) Recommendations. World Health Organisation, September 2017.

WHO, 2022. Guidelines for drinking-water quality, 4th edition. Incorporating the first and second addenda, 4th ed + 1st add + 2nd add. WHO.

Zhang, J., Tejada-Martínez, A.E., Zhang, Q., Lei, H., 2014. Evaluating hydraulic and disinfection efficiencies of a full-scale ozone contactor using a RANS-based modelling framework. Water Res. 52, 155–167.